Mol. Cells 2015; 38(10): 876-885
http://dx.doi.org/10.14348/molcells.2015.0120

Molecules and Cells
http://molcells.org
Established in 1990

N-Acetyl-*D*-Glucosamine Kinase Promotes the Axonal Growth of Developing Neurons

Md. Ariful Islam[1], Syeda Ridita Sharif[1], HyunSook Lee[2], and Il Soo Moon[1,2,*]

***N*-acetyl-*D*-glucosamine kinase (NAGK) plays an enzyme activity-independent, non-canonical role in the dendritogenesis of hippocampal neurons in culture. In this study, we investigated its role in axonal development. We found NAGK was distributed throughout neurons until developmental stage 3 (axonal outgrowth), and that its axonal expression remarkably decreased during stage 4 (dendritic outgrowth) and became negligible in stage 5 (mature). Immunocytochemistry (ICC) showed colocalization of NAGK with tubulin in hippocampal neurons and with Golgi in somata, dendrites, and nascent axons. A proximity ligation assay (PLA) for NAGK and Golgi marker protein followed by ICC for tubulin or dynein light chain roadblock type 1 (DYNLRB1) in stage 3 neurons showed NAGK-Golgi complex colocalized with DYNLRB1 at the tips of microtubule (MT) fibers in axonal growth cones and in somatodendritic areas. PLAs for NAGK-dynein combined with tubulin or Golgi ICC showed similar signal patterns, indicating a three way interaction between NAGK, dynein, and Golgi in growing axons. In addition, overexpression of the *NAGK* gene and of kinase mutant *NAGK* genes increased axonal lengths, and knockdown of NAGK by small hairpin (sh) RNA reduced axonal lengths; suggesting a structural role for NAGK in axonal growth. Finally, transfection of 'DYNLRB1 (74-96)', a small peptide derived from DYNLRB1's C-terminal, which binds with NAGK, resulted in neurons with shorter axons in culture. The authors suggest a NAGK-dynein-Golgi tripartite interaction in growing axons is instrumental during early axonal development.**

INTRODUCTION

N-acetylglucosamine (GlcNAc), a core component of different complex carbohydrates, is synthesized *de novo*, or derived from the lysosomal degradation of oligosaccharide moieties. *N*-acetylglucosamine kinase (NAGK; EC 2.7.1.59), is the key enzyme in the metabolic route responsible for recycling GlcNAc into GlcNAc 6-phosphate. GlcNAc 6-phosphate may then enter a catabolic route that links hexosamine metabolism with the glycolytic pathway (Wolosker et al., 1998) or may enter an anabolic pathway leading to UDP-GlcNAc formation (Reutter et al., 1997). The activated sugar nucleotide UDP-GlcNAc is a substrate for the synthesis of the oligosaccharide chains of *N*- and *O*-glycans and glycolipids (Hakomori, 2000; Schachter, 2000; Van den Steen et al., 1998), glycosaminoglycans, and the glycosylphosphatidylinositol anchor of membrane-bound glycoproteins (Esko and Lindahl, 2001; Hwa, 2001; Watanabe et al., 2000). Hinderlich et al. (1998) purified NAGK from rat liver and reported that it forms homodimers of 37-kDa subunits in solution, whereas NAGK of human origin forms homodimers of 39-kDa subunits. In 2000, Hinderlich et al. cloned human and mouse NAGK genes and showed NAGK is a member of the *N*-acetylhexosamine kinase family, which are in turn members of the sugar kinase/heat shock protein 70/actin superfamily (Berger et al., 2002). Subsequently, Weihofen et al. (2006) determined crystal structures of homodimeric human NAGK complexed with GlcNAc or with ADP and glucose.

In contrast to detailed studies on the enzyme itself, the expressions and functions of NAGK in mammalian tissues have been little studied. Northern and Western blot analyses showed that NAGK mRNA and protein are expressed in different cell lines and tissues (Hinderlich et al., 2000). More recently, our lab reported a non-canonical function of NAGK in neuronal dendritogenesis. More specifically, exogenous NAGK overexpression was found to upregulate dendritic arborization, and the small domain of NAGK was identified as the key epitope. Furthermore, knockdown of the NAGK with NAGK-shRNA reduced dendritic arborization (Lee et al., 2014a), and the dendritogenetic effect role of NAGK was later found to be independent of its kinase activity (Lee et al., 2014b). Sharif et al. (2015) described the expression of NAGK in different subnuclear compartments, such as, speckles and paraspeckles, and on the outer nuclear membrane. Our lab also reported that NAGK interacts with several intracellular proteins, including, dynein light chain roadblock type-1 (DYNLRB1), small nuclear ribonucleoprotein-associated protein N (snRNPN), p54NRB, and a general transcription factor IIH polypeptide 5 (GTF2H5) (Islam et al., 2015; Sharif et al., 2015). We also reported the functional role played by the NAGK-DYNLRB1 interaction during dendrite development, which is noteworthy because it is associated with somatic Golgi stacks and dendritic Golgi outposts (Islam et al., 2015). In total, these findings indicate that NAGK plays a critical role in neuronal development.

[1]Department of Anatomy, [2]Dongguk Medical Institute, College of Medicine Dongguk University, Gyeongju 780-714, Korea
*Correspondence: moonis@dongguk.ac.kr

Received 7 May, 2015; revised 3 August, 2015; accepted 5 August, 2015; published online 15 October, 2015

Keywords: axon, dynein, Golgi, microtubule, NAGK, neuron

eISSN: 0219-1032

Axons and dendrites differ from one another in morphology and function. A series of time-lapse video microscopic studies using low density cultures of hippocampal neurons (Dotti et al., 1988; Goslin and Banker, 1990; Goslin et al., 1998) revealed a stereotypic sequence of characteristic morphological changes. Shortly after attachment to substratum, cell peripheries become flattened to produce lamellipodia (developmental stage 1; the lamellipodia stage). Within several hours, short processes of roughly equal length emerge (stage 2; the minor process stage). At this stage processes cannot be identified as axonal or dendritic, and typically, over the next 12-24 h, undergo net elongation, during which minor processes extend or retract dynamically for short distances. After this apparent latent period, one of the minor processes on a cell begins to grow rapidly and acquires axonal characteristics within hours (stage 3; the axonal outgrowth stage). This stage lasts several days during which axons continue to grow, while the net lengths of other minor processes do not elongate. These minor processes begin to elongate at a significantly slower rate than axons and become dendrites (stage 4; the dendritic outgrowth stage). When dendritic outgrowth is complete neurons are fully polarized and mature (stage 5; the mature stage). In this study, we studied the role played by NAGK in axonal development by investigating immunoreactivity signals during each of these stages.

MATERIALS AND METHODS

Antibodies and plasmids

The following antibodies were used at the indicated dilutions unless otherwise mentioned: chicken polyclonal NAGK (1:1000 for ICC; GenWay Biotech, Inc., now GW22347, Sigma, USA); mouse monoclonal NAGK (1:10 for PLA; Santa Cruz Biotechnology Inc., Dallas, TX); rabbit polyclonal NAGK (1:50 for PLA; GeneTex, USA); rabbit polyclonal DYNLRB1 (1:25; Proteintech Group, Inc., USA), rabbit polyclonal dynein heavy chain (1:25; Santa Cruz); mouse monoclonal TGN38 (1:50; BD Biosciences, USA); rabbit polyclonal GM130 (1:25; Santa Cruz); mouse monoclonal alpha tubulin (1:10; broth preparation, Developmental Studies Hybridoma Bank, University of Iowa, USA); and mouse monoclonal Ankyrin G (1:50, Santa Cruz). The plasmids used for transfection were pDsRed2 vector, pDsRed2-tagged wild-type NAGK, pEGFP-tagged point mutants of NAGK (-N36A, -D107A, and -C143S), and NAGK short hairpin (sh) RNA, all as previously described (Lee et al., 2014a; 2014b).

Primary culture

Hippocampi from embryonic day 19 (E19) Sprague-Dawley rat pups were dissected, dissociated with trypsin and mechanical trituration, and plated onto 12-mm diameter polylysine/laminin coated glass coverslips at a density of ~150 neurons/mm^2, as previously described (Brewer et al., 1993). Cells were initially plated in MACS® Neuro Medium (Miltenyi Biotec Inc., USA) supplemented with MACS NeuroBrew®-21, 45.95 μM glutamate, 500 μM glutamine, 25 μM 2 mercaptoethanol, and 1% penicillin-streptomycin, and fed every 4 days after plating with the same media (without additional glutamate or 2-mercaptoethanol).

DNA and peptide transfection

Hippocampal neurons were transfected with plasmid using Lipofectamine® 2000 reagent (Invitrogen, USA) according to the manufacturer's instructions. An 18-amino acid peptide termed 'DYNLRB1 (59-76)' and a 23-amino acid peptide termed 'DYNLRB1 (74-96)', which were both derived from the NAGK-binding region of DYNLRB1, were custom made by Anygen (Korea) at a purity of 98%. Peptide transfection was performed in neurons after 24 h of plating with a Chariot protein transfection kit (Active Motif, California) using a modified version of the manufacturer's instructions as previously described (Islam et al., 2015). After incubation for 48 h, neurons were fixed and stained using a β-galactosidase staining kit (Active Motif).

Immunocytochemistry (ICC)

Cells were fixed using a sequential paraformaldehyde/methanol fixation procedure [incubation in 4% paraformaldehyde in phosphate buffered saline (20 mM sodium phosphate buffer, pH 7.4, 0.9% NaCl) at room temperature (RT) for 10 min followed by incubation in 100% methanol at -20°C for 20 min] (Moon et al., 2007). ICC was performed with the indicated primary and secondary [Alexa Fluor 488/568/647-conjugated goat anti-mouse/rabbit/chicken (each diluted 1:1,000 in blocking buffer; Invitrogen)] antibodies, as previously described (Moon et al., 2007).

Proximity ligation assay (PLA)

Generic *in situ* PLA was conducted using a Duolink In Situ kit (Olink Bioscience, Sweden) using a modified version of the manufacturer's instructions and as described by Islam et al. (2015). Briefly, after incubating fixed cells with primary antibodies overnight at 4°C, secondary antibodies conjugated with oligonucleotides, PLA probe anti-mouse MINUS and PLA probe anti-rabbit PLUS, were added and incubated for 2 h at 37°C in a humidity chamber. Cells were then treated with ligation mixture and ligase at 37°C for 30 min, and after hybridization and ligation of DNA oligonucleotides, an amplification solution and polymerase were added. Amplified products were detected using complimentary fluorescently labeled oligonucleotides. For combined proximity ligation assays (PLAs) and immunocytochemistry (ICC), PLA reactions were performed first, and then primary antibodies were added to the cells, which were then incubated overnight at 4°C, and subsequently incubated with fluorophore-conjugated secondary antibodies described in the ICC procedure above.

Image acquisition and analysis

A Leica Research Microscope (DM IRE2) equipped with I3 S, N2.1 S, and Y5 filter systems (Leica Microsystems AG, Germany) was used for epifluorescence microscopy. Images (1388 x 1039 pixels) were acquired using a high-resolution CoolSNAP CCD camera (Photometrics Inc., USA) and Leica FW4000 software. Digital images were processed using Adobe Systems Photoshop 7.0 software (Adobe, USA). Axonal lengths were measured with Image J (version 1.45) software using the simple neurite tracer plug-in (National Institute of Health, USA).

Statistics

Data were analyzed using one-way analysis of variance (ANOVA) and Duncan's multiple comparison as a *post hoc* test. Statistical significance was accepted for p values of < 0.01, and the analysis was conducted using SPSS version 16.0 (SPSS Inc., USA).

RESULTS

NAGK was present throughout neurons until developmental stage 3

To investigate the spatiotemporal expression of NAGK, we

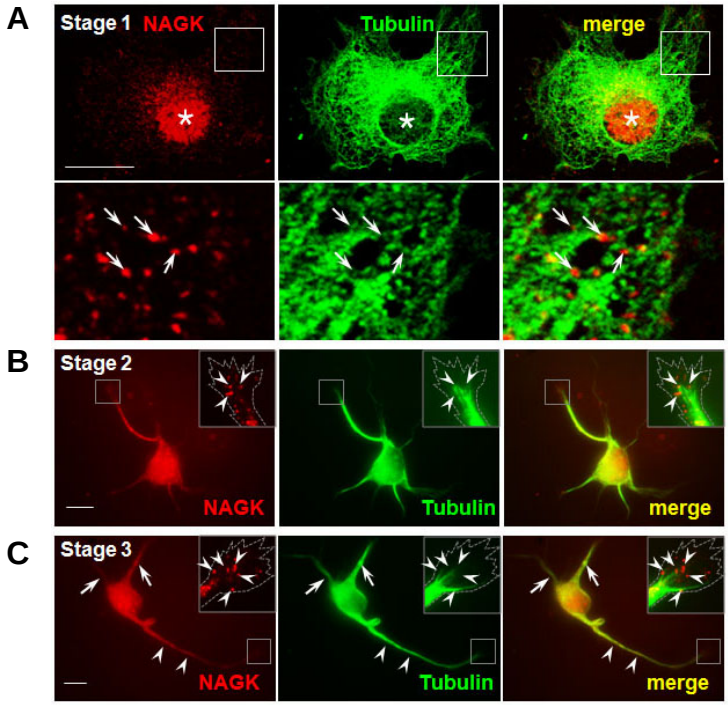

Fig. 1. Expressions of NAGK in developmental stage 1, 2 and 3 neurons. Rat hippocampal neurons in culture were double-labeled with NAGK (red) and tubulin (green). (A) Stage 1 (lamellipodia). (B) Stage 2 (minor process). (C) Stage 3 (axonal outgrowth). (A) Strong nuclear NAGK expression is marked with asterisks and boxed areas are enlarged below to show the expression of NAGK on MTs at initial neuronal extensions (arrows). (B) The growth cone from a minor process is marked with box and enlarged (*inset*) to show the expression of NAGK at the tips of MT fibers (arrowheads). (C) Axon and dendrites are indicated by arrowheads and arrows, respectively. The growth cone of a developing axon is marked with box and enlarged (*inset*) to show the expression of NAGK at the edges of neonate MT fibers (arrowheads). Scale bar; 10 μm.

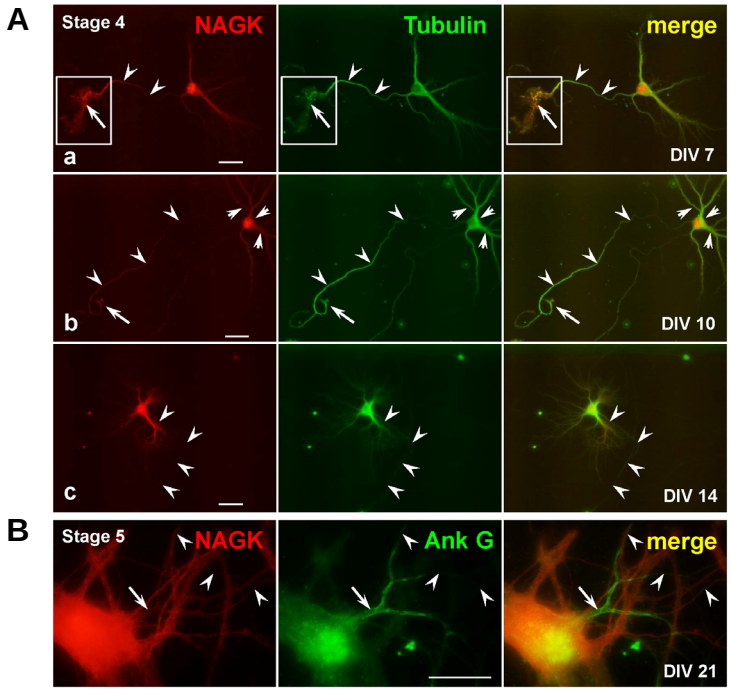

Fig. 2. Expression of NAGK in developmental stage 4 (dendritic growth) and 5 (mature) neurons. (A) Stage 4 neurons. Epifluorescence microscopic images showing the expression profile of NAGK in sub-stages of Stage 4. In early Stage 4 (DIV7; a), the axonal growth cone is large (arrow) and NAGK levels in the axonal shaft (arrowheads) and growth cone remain high. However, as neurons matured (DIV10, b), the sizes of axonal growth cones (arrow) reduced and shafts (arrowheads) tightened. Note that the expression level of NAGK is significantly lower in (A-b) than in (A-a). In late stage 4 neurons (DIV14, c), the axonal expression of NAGK was reduced further. (B) A mature stage 5 neuron (DIV21). The axon was identified by staining with an antibody against ankyrin G (Ank G). Note that the expression level of NAGK is very low in the axon initial segment (arrow) and in its shaft (arrowheads). Scale bar, 30 μm.

double-labeled cultured hippocampal neurons in the early developmental stages with anti-NAGK and anti-tubulin antibodies. NAGK expression was observed in cell bodies and protrusions in developmental stages 1, 2, and 3 neurons as shown in Figs. 1A, 1B, and 1C, respectively. NAGK was highly expressed from the beginning of morphological differentiation (stage 1, lamellipodia) and highest immunoreactivity (IR) was observed in nuclei (Fig. 1A, asterisks). Immunostaining revealed discrete clusters in perikaryon and density gradients from nuclei to cell peripheries where NAGK colocalized with tubulin-IR signals (Fig. 1A, enlarged boxed area, arrows). In stage 2 neurons, NAGK-IR was strong in nuclei and IR clusters were distributed in somata, minor processes, and growth cones (Fig. 1B), where it colocalized with tubulin-IR (inset, arrowheads). In stage 3 (axonal outgrowth, Fig. 1C) neurons, which showed distinct, long axonal processes, NAGK was highly expressed in dendrites (arrows) and axons (arrowheads), in which NAGK-IR was colocalized with the distal tips of MTs in axonal growth cones

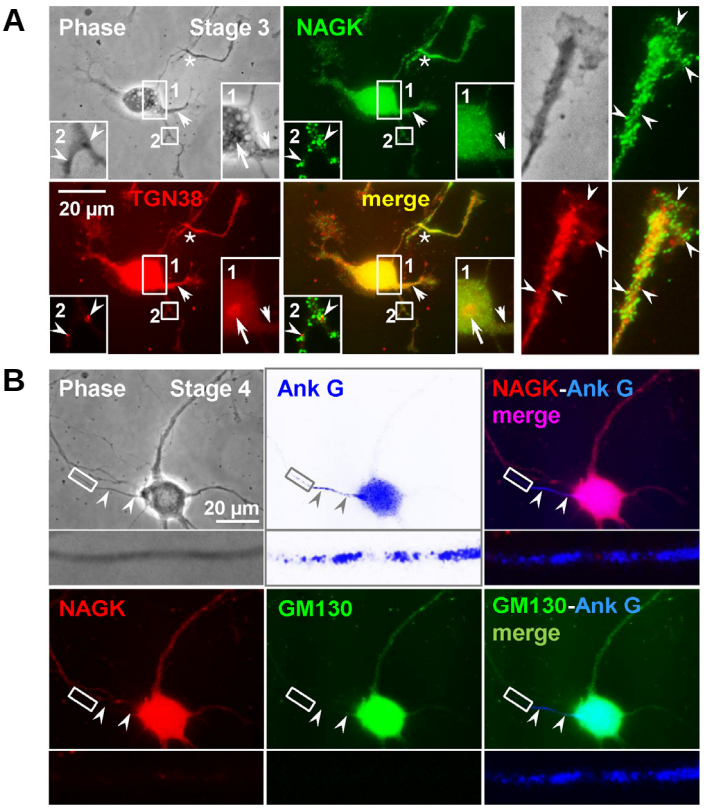

Fig. 3. The presences and absences of NAGK and Golgi during axon development. (A) Colocalization of NAGK and Golgi in the axon of a stage 3 neuron. NAGK and Golgi were visualized *in situ* in development stage 3 hippocampal neurons by double staining with anti-TGN38 (red) and anti-NAGK (green) antibodies. In the cell body several NAGK signals overlap with the compact cluster-like signals of Golgi complex (*inset* 1, long arrows) oriented toward an apical dendrite (short arrows). In growing neurites, Golgi extended as discrete Golgi particles far into dendritic shafts at branch points (*inset* 2, arrowheads), axonal shafts (asterisks), and axonal growth cone (enlarged right side, arrowheads) and colocalized with NAGK immunoreactivity. Scale bar, 20 μm. (B) Absence of NAGK and Golgi in the axon of a stage 4 neuron. NAGK, Golgi, and the axonal initial segment are marked by anti-NAGK, anti-GM130, and anti-ankyrin G (Ank G) antibody triple staining. NAGK and Golgi images are merged with an ankyrin G image and a portion of the axonal shaft is enlarged (*inset*). NAGK and Golgi outposts were both absent in axons marked with ankyrin G signals (arrowheads). Scale bar, 20 μm.

(*inset*, arrowheads). In the stage 3, axonal and dendritic NAGK-IR intensities were comparable, indicating that NAGK was distributed equally in these two compartments.

NAGK expression in the axons decreased abruptly from developmental stage 4

In stage 4 (dendritic outgrowth) neurons, dendrites start to grow in length and axons mature to produce their characteristic shape. At this stage, we fixed hippocampal neurons at three different culture time points (i.e., DIV7, DIV10, and DIV14), and double-labeled with anti-NAGK and anti-tubulin antibodies. At DIV7, we observed NAGK signals in axonal shafts (Fig. 2A-a, arrowheads) and growth cones (box with an arrow). At DIV 10 (Fig. 2A-b), axons had extended further and growth cones were smaller (arrow). During maturation, NAGK expression in axons decreased significantly (Fig. 2A-b, arrowheads), but it did not do so in the somatodendritic domain (Fig. 2A-b, short arrows). Later in stage 4 (DIV14), NAGK-IR was barely seen in axons (Fig. 2A-c, arrowheads), which by then had developed typical axon-like features. This observed gradual decline in NAGK expression in axons suggests that NAGK's function in this compartment becomes less important as neuronal development progresses.

Mature neurons (stage 5) are highly complex with multiple branched dendrites and a thin long axon, which is difficult to identify by shape. Therefore, we double-stained stage 5 (DIV21) neurons with anti-NAGK and anti-ankyrin G, markers of the axon initial segment (Fig. 2B). NAGK-IR was barely found in mature axons (arrowheads), which showed strong ankyrin G-IR (arrow). The absence of NAGK in the axons of mature neurons (stage 5) suggests that NAGK is required during development but not by mature axons.

Both NAGK and Golgi outposts were present in growing axons but absent in mature axons

The neuronal Golgi apparatus is basically composed of Golgi stacks in the cell body and discrete Golgi 'outposts' in dendrites. Golgi outposts are excluded from mature axons (Horton and Ehlers, 2003; Horton et al., 2005), but are present in growing axons (Estrada-Bernal et al., 2012; Merianda et al., 2009). To determine the relative distribution profiles of NAGK and Golgi in axons, we double stained stage 3 neurons (axonal outgrowth stage) with anti-NAGK (green) and anti-Trans Golgi Network protein 38 (TGN38, red) antibodies (Fig. 3A). We observed typical Golgi stacks in somal regions (TGN38, *inset* 1, long arrow) oriented toward the apical dendrite (*inset* 1 and original image, short arrows) and discrete Golgi signals in axons with higher frequencies in growth cones. NAGK signals in these axons were patch-like. Interestingly, Golgi signals frequently colocalized with NAGK signals in axonal shafts (asterisks), growth cones (enlarged right side, arrowheads), and in dendrites, particularly at branch bifurcation points (*inset* 2, arrowheads).

We then triple stained stage 4 neurons with anti-NAGK, anti-Golgi Matrix protein 130 (GM130), and anti-ankyrin G antibodies (Fig. 3B). Ankyrin G signal marked axons (arrowheads) where Golgi signals (GM130) were absent and NAGK expression was barely observed (enlarged *insets*). This co-existing expression pattern in different time frame of neuronal development indicates a spatiotemporal functional connection between NAGK and Golgi.

NAGK, Golgi, and DYNLRB1 colocalized in axons

We previously showed that NAGK interacts with DYNLRB1 and NAGK-dynein-Golgi tripartite interactions occur in somata and dendrites, especially in dendritic branch points in stage 4 neurons,

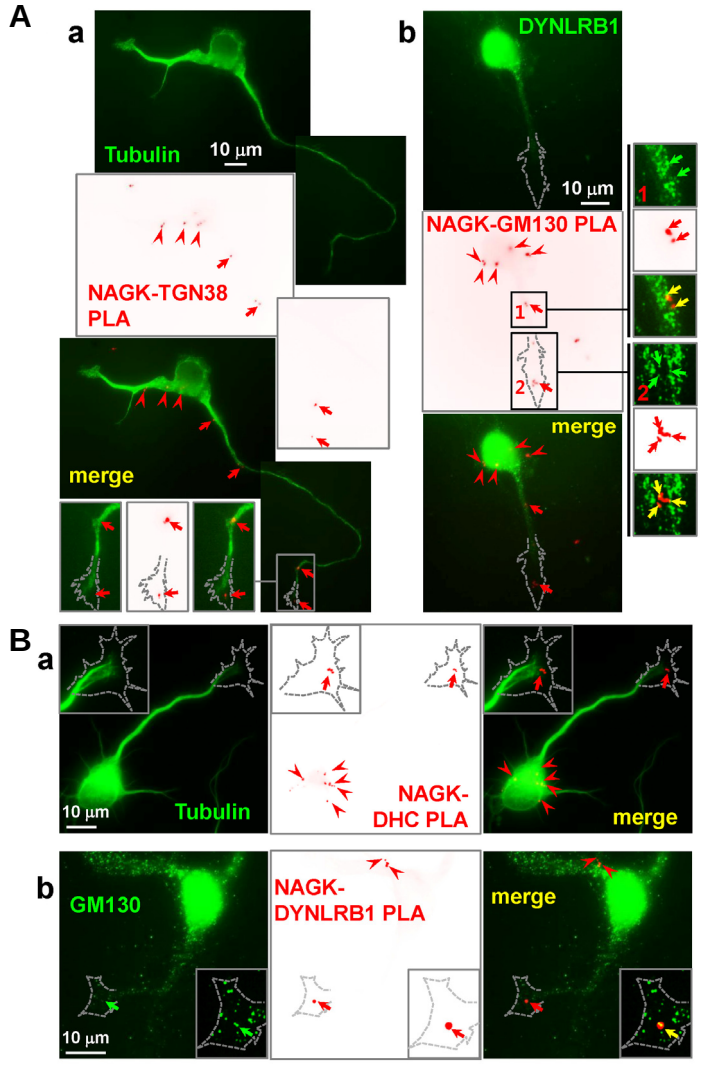

Fig. 4. NAGK-dynein-Golgi tripartite interaction in growing axons. (A) Interaction between NAGK and Golgi in growing axons. NAGK-TGN38 PLA was performed on stage 3 hippocampal neurons and followed by ICC using anti-tubulin (green) antibody (a). PLA signals in the somatodendritic domain (arrowheads) and in axons (arrows) are indicated by red dots and are merged with tubulin signals. A typical axonal growth cone is enlarged in the *inset* to show the NAGK-Golgi interaction (arrows) at the distal end of an MT. Scale bar, 10 μm. Next, NAGK-GM130 PLA combined with DYNLRB1 ICC was conducted (b). Red PLA dots defining NAGK-Golgi interactions at somata (arrowheads), axonal shafts (arrow 1) and growth cones (arrow 2) are shown. PLA signal positions in an enlarged axon (*inset*) show the colocalization of NAGK-Golgi PLA signals and DYNLRB1 signals (arrows). Scale bar, 10 μm. (B) Interaction between NAGK and dynein in a growing axon. NAGK-DHC PLA was performed on fixed hippocampal neurons, which were then immunostained with anti-tubulin (green) antibody (a). NAGK-dynein interactions are shown as red PLA signals in somata (arrowheads) and in axonal growth cones (arrow). An axonal growth cone is enlarged (*inset*) to show NAGK-dynein complex at the tip of MTs (arrow). Scale bar; 10 μm. NAGK-DYNLRB1 PLA signals (red) were colocalized with GM130 signals (green) in dendrites (arrowheads) and in axonal growth cones (b, arrows, enlarged *inset*). Scale bar, 10 μm.

and that the NAGK-DYNLRB1 interaction is critical during dendritogenesis (Islam et al., 2015). To investigate NAGK-dynein-Golgi colocalization in axons, we conducted a proximity ligation assay (PLA) using anti-NAGK and anti-TGN38 antibodies followed by ICC with anti-tubulin antibody in stage 3 hippocampal neurons (Fig. 4A-a). We found PLA signals (red dots), representing NAGK-Golgi interactions, in somatodendritic compartments (arrowheads) and in axonal shafts and growth cones (arrows). Tubulin staining revealed that the NAGK-Golgi interaction often occurred at axonal branch initiation sites having dispersed MT fibers and at the distal tips of MTs in growth cones (*inset*, arrows). Next, we conducted NAGK-GM130 PLA followed by ICC for DYNLRB1 and found NAGK-Golgi interaction (Fig. 4A-b, PLA) in somata (arrowheads), axonal shafts (arrow 1) and growth cones (arrow 2) and PLA signals colocalized with DYNLRB1 signals in axons (*insets*, arrows).

To confirm the colocalization of NAGK-Golgi interaction with dynein, we conducted PLA with anti-NAGK and anti-dynein heavy chain (DHC) antibodies followed by ICC using anti-tubulin antibody in stage 3 hippocampal neurons (Fig. 4B-a). NAGK-DHC interactions were found in somatic peripheral areas (arrowheads) where Golgi could be present and at the distal end of MTs in axonal growth cones (arrows). Supporting this result, NAGK-DYNLRB1 PLA followed by staining with anti-GM130 antibody in stage 3 neurons showed NAGK-dynein interactions in dendrites (Fig. 4B-b, arrowheads) and axonal growth cones (arrows) where PLA signals colocalized with GM130 signals (*inset*, arrows). These results show NAGK interacted with DYNLRB1 in association with Golgi outposts in growing axons, and suggest a molecular mechanism for NAGK during the development of axons.

Exogenous NAGK overexpression upregulated and NAGK knockdown delayed axonal growth

To investigate the functional role of NAGK in axons, we transfected hippocampal neurons at the early stage of neuronal development (i.e., DIV 1) with a red fluorescent protein tagged NAGK plasmid (Fig. 5A-a, pDsRed2-NAGK), with pDsRed2 control plasmid alone (Fig. 5A-b, pDsRed2/Control), or co-transfected with NAGK shRNA plasmid (Fig. 5A-c, pDsRed2 + sh-NAGK). After incubation for 48 h transfected neurons were bright red indicating the presence of exogenous proteins. We then measured axonal lengths and plotted then on a line graph (Fig. 5B-a, n = 50). To visualize axonal growth, we plotted numbers of neurons with different axonal lengths on a line graph (Fig. 5B-b). Average axonal lengths of NAGK shRNA,

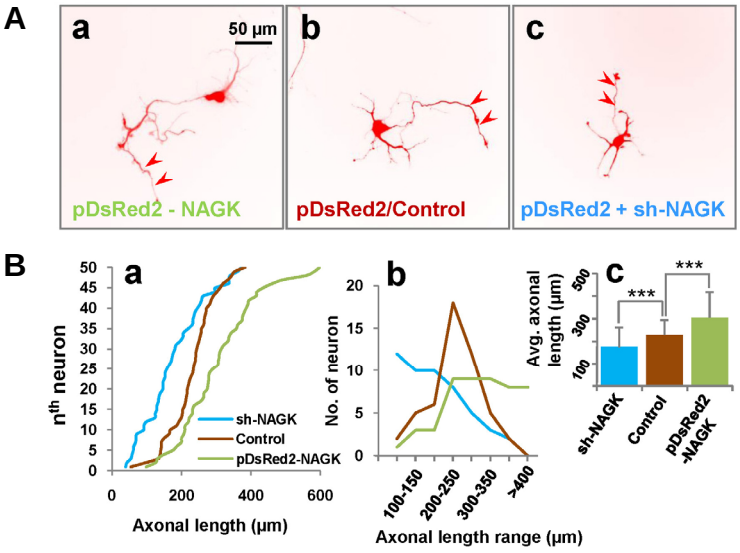

Fig. 5. NAGK overexpression increased axon lengths and NAGK knockdown reduced lengths. Hippocampal neurons (DIV 1) were transfected with indicated plasmids and images were acquired after incubation for 48 h. (A) Epifluorescent live cell images showing neurons transfected with the indicated plasmids. Neurons transfected with DsRed2 tagged NAGK plasmid (pDsRed2 - NAGK) had longer axons (a, arrowheads), and neurons co-transfected with DsRed2 and NAGK shRNA (sh-NAGK) had shorter axons (c, arrowheads) than DsRed2 transfected controls (b, arrowheads). Scale bar; 50 μm. (B) Statistics. Axonal lengths of transfected neurons are plotted on a line graph in ascending order (a). Numbers of neurons with axonal lengths in different ranges with the increment of 50 μm are plotted on the line graph for comparison purposes (b). Average axonal lengths were also compared using a bar diagram (c), which shows neurons provided exogenous NAGK (pDsRed2 - NAGK) had significantly longer axons and neurons treated with NAGK shRNA (sh-NAGK) had significantly shorter axons than the pDsRed2 transfected control. ***$p < 0.01$, n = 50.

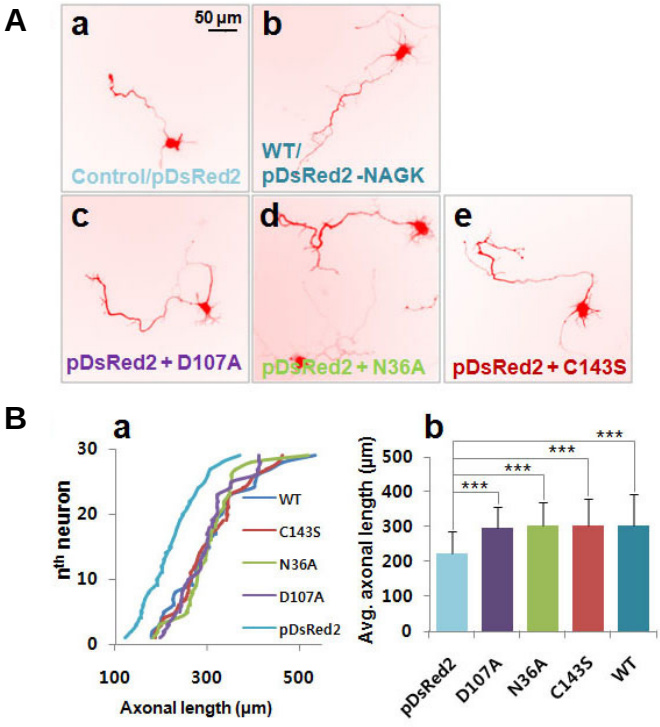

Fig. 6. NAGK point mutants with differential kinase activities similarly promoted axonal growth. (A) Epifluorescence images of typical neurons expressing control pDsRed2 vector plasmid (a), pDsRed2-tagged WT (b), or D107A (c), N36A (d), or C143S (e) mutant NAGKs cotransfected with pDsRed2. Scale bar, 50 μm. (B) Statistics. Line graph showing axonal lengths of transfected neurons in ascending order (a). Average axonal lengths of pDsRed2 control, D107A, N36A, C143S and pDsRed2-tagged WT group are presented as a bar diagram for comparison (b), which shows neurons provided exogenous WT NAGK or NAGK point mutants (N36A, D107A, or C143S) all had significantly longer axons than pDsRed2 controls. ***$p < 0.01$, n = 30.

pDsRed2 control and pDsRed2-NAGK transfected cells were plotted on a bar diagram (Fig. 5B-c). Neurons transfected with pDsRed2-NAGK plasmid had significantly longer axons (average length 307.28 μm, increased by 33.18%) than pDsRed2 plasmid transfected controls (average length 230.72 μm) ($p < 0.01$). Conversely, neurons transfected with NAGK shRNA plasmid had significantly shorter axons (average length 175.48 μm, decreased by 23.94%) than pDsRed2 plasmid transfected controls ($p < 0.01$). These results indicate that NAGK is essential for axonal growth during the early developmental stage.

NAGK promoted axonal growth independent of its kinase activity

To study the connection between axonal growth and the kinase activity of NAGK, we utilized three previously designed point mutant NAGK plasmids, that is, N36A, D107A, and C143S. The D107A mutation almost completely abrogates the kinase activity of NAGK, whereas the C143S and N36A mutations retain 75% and 49% of WT NAGK activity, respectively (Lee et al., 2014b). When these plasmids were introduced by transfection into DIV 1 hippocampal neurons in culture, the overexpression of these mutant NAGKs did not impede neuronal growth,

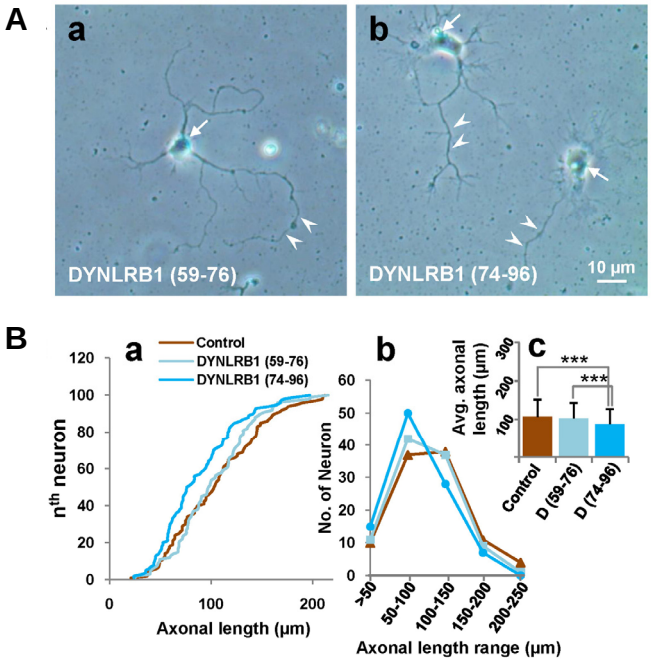

Fig. 7. Transfection with a small peptide from DYNLRB1 delayed axonal growth. (A) Typical images of transfected neurons. Stage 1 hippocampal neurons were co-transfected with either 'DYNLRB1 (59-76)' or 'DYNLRB1 (74-96)' peptide and β-galactosidase, incubated for 48 h and then stained using a β-galactosidase staining kit. Transfected cells were identified by a characteristic blue color (arrows). Neurons transfected with 'DYNLRB1 (59-76)' (a, arrowheads) routinely developed long axons, but 'DYNLRB1 (74-96)' treated neurons had shorter axons (b, arrowheads) than the control. Scale bar, 10 μm. (B) Statistics. Axonal lengths in ascending order (a), numbers of axons with in different length ranges (b), and average axonal lengths (c) of neurons transfected with β-galactosidase or co-transfected with β-galactosidase and 'DYNLRB1 (59-76)' or 'DYNLRB1 (74-96)' are plotted. 'DYNLRB1 (59-76)' and 'DYNLRB1 (74-96)' are referred to as 'D (59-76)' and 'D (74-96)', respectively, in the bar diagram (c). 'DYNLRB1 (74-96)' transfected neurons had significantly shorter axons than the β-galactosidase transfected control. ***$p < 0.01$, n = 100.

but rather resulted in neurons with longer axons. Typical images of live neurons transfected with pDsRed2 control vector (Fig. 6A-a), pDsRed2-NAGK-WT (Fig. 6A-b), and of neurons co-transfected with pDsRed2 vector plasmid and -D107A (Fig. 6A-c), or -N36A (Fig. 6A-d) or -C143S (Fig. 6A-e) mutant NAGKs are shown in Fig. 6A. After 48 h of incubation, images of live transfected neurons were captured using a fluorescence microscope. Differences between axonal lengths were compared by plotting lengths on a line graph (Fig. 6B-a, n = 30) and average lengths using a bar diagram (Fig. 6B-b). The lengths of axons in neurons transfected with mutant NAGKs (N36A, D107A, C143S) or with WT NAGK were significantly longer ($p < 0.01$) than those transfected with the pDsRed2 vector control. Furthermore, these mutants and the WT showed no difference in this respect, which suggests the role of NAGK during axonal development is non-enzymatic in nature.

Inhibition of the NAGK-DYNLRB1 interaction downregulated axonal growth

In our previous study, we showed that transfection of a small peptide, 'DYNLRB1 (74-96)' (KKNEIMVAPDKDYFLIVIQNPTE) from the C-terminal part of DYNLRB1, which binds with NAGK, resulted in stunted dendrites in stage 4 neurons (Islam et al., 2015). To determine whether a similar phenomenon occurs during axonal development, stage 1 hippocampal neurons were co-transfected with 'DYNLRB1 (74-96)' or 'DYNLRB1 (59-76)' (EIDPQNDLTFLRIRSKKN) plus β-galactosidase, or with β-galactosidase alone. Transfected neurons were identified using the β-galactosidase reaction, which produces a characteristic blue color (Fig. 7A, arrows). Neurons transfected with the control peptide 'DYNLRB1 (59-76)' freely extended their axons identified as the longest neurite at this stage of neuronal development (Fig. 7A-a, arrowheads). On the other hand, neurons transfected with 'DYNLRB1 (74-96)' had shorter axons (Fig. 7A-b, arrowheads). We measured axonal lengths of 'DYNLRB1 (74-96)', 'DYNLRB1 (59-76)', and β-galactosidase control groups and plotted results on a line graph in ascending order (Fig. 7B-a, n = 100), and also studied axonal lengths of these three treatment groups using a length range plot (Fig. 7B-b). By comparing average axonal lengths on a bar diagram (Fig. 7B-c), it was found that the axons of 'DYNLRB1 (74-96)' treated neurons had an average length of 87.18 μm, which was significantly ($p < 0.01$) shorter than those of 'DYNLRB1 (59-76)' treated neurons or 'β-galactosidase' treated controls that had average axon lengths of 102.17 μm and 105.67 μm, respectively. These results confirm that interruption of the NAGK-DYNLRB1 interaction results in delayed axonal growth.

DISCUSSION

In this paper, we report that NAGK was highly expressed in neurons from the beginning of the morphological development and distributed throughout cells until developmental stage 3 (the axonal outgrowth stage), and that subsequently, the axonal expression of NAGK dramatically reduced. These observations show that NAGK is redistributed in neurons during the developmental process. In addition, the study confirms a NAGK-dynein-Golgi tripartite interaction in growing axons, and hints at the functional role of NAGK during axonal growth.

We also found that NAGK colocalizes with Golgi outposts in growing axons, which is interesting because the existence of Golgi complexes in axons has been questioned for a considerable time. Initially, it was reported that Golgi are present in neurons as a central Golgi compartment in somata and as small Golgi 'outposts' in dendrites (particularly at dendritic branch points), but are not present in axons (Gardiol et al., 1999; Horton and Ehlers, 2003; Horton et al., 2005; Pierce et al., 2001). This notion was challenged when screening for an all-inclusive list of proteins available in axonal growth cones was performed by extensive proteomic analysis (Estrada-Bernal et al., 2012) where Golgi related protein clusters and dynein complex were found in axonal growth cones. Merianda et al. (2009) also showed that the growing axons of cultured rat dorsal root ganglion (DRG) neurons contain ER and Golgi components needed for classical protein synthesis and secretion. Moreover, treatment of hippocampal neurons in culture with brefeldin A (which reversibly disrupts the Golgi complex) was observed to inhibit axonal growth (Jareb and

Banker, 1997). These findings appear to be sufficient to conclude Golgi is present in growing axons and that it is involved in axonal growth. Our results strengthen this conclusion by showing that Golgi specific proteins, such as, TGN38 and GM130, localize to the growing axonal shafts and growth cones of stage 3 hippocampal neurons in culture.

Furthermore, our PLA assay revealed NAGK-Golgi interactions in growing axons. In particular, we observed interactions between NAGK and GM130 (a *cis*-Golgi marker protein) and with TGN38 (a *trans*-Golgi marker protein) in somal Golgi compartments and in growing axons (mostly at growth cones). We also found NAGK-Golgi complexes interact with DYNLRB1, suggesting a NAGK-Golgi-dynein three way interaction in stage 3 axons. DYNLRB1 is a member of multiprotein dynein motor complex and belongs to the LC7/Roadblock family of light chains (LCs). In *Drosophila melanogaster*, LC7-null mutants exhibited defective axonal transport (Reuter et al., 2003), and in rat sympathetic neurons siRNA knockdown of DHC resulted in reduced axon length (Ahmad et al., 2006) while treatment with ciliobrevin D, a pharmacological dynein inhibitor, reversibly inhibited axonal growth in chicken dorsal root ganglion neurons (Sainath and Gallo, 2014). In the present study, we observed similar patterns of axonal growth in early stage neurons, that is, NAGK-shRNA transfection resulted in shorter axons and augmentation with exogenous NAGK yielded significantly longer axons. Furthermore, our findings indicate the role of NAGK in axonal growth is independent of its enzymatic function, because NAGK point mutants with variable enzymatic activity promoted axonal growth as effectively as the wild type, indicating a structural role for NAGK in axonal growth. In our previous study, we reported the NAGK-dynein interaction and that the inclusion of 'DYNLRB1 (74-96)' (a small peptide segment of the DYNLRB1 protein sequence containing a potential binding epitope for NAGK) into stage 4 hippocampal neurons resulted in stunted dendritic arbors (Islam et al., 2015). Interestingly, the axons of neurons in this previous study were seemingly unaffected, which is in-line with the very low level of NAGK expression in mature axons observed in the present study. On the other hand, similar experiments with early stage neurons in the present study, showing strong NAGK expression in nascent axons, resulted in delayed axonal growth. These observations indicate 'DYNLRB1 (74-96)' interacts with and interferes with the function of NAGK during axonal development. Since dynein is a molecular motor that enables transport toward the minus-ends of MTs, these findings suggest that NAGK regulates dynein motor function in the Golgi transport system in neuronal axons and dendrites.

We also observed a large variation in the axonal lengths of neurons in cultures expressing exogenous RFP (Figs. 5 and 6) and β-galactosidase (Fig. 7). Axons grow rapidly in stage 3 (axonal outgrowth), and according to Dotti et al. (1988) in this stage axon-to-stomata lengths reach 40 μm after 1 day in culture and then elongate by about 70 μm/day for the next few days. A small due to difference in the time schedule between experiments may have resulted in axonal length differences, although it is also possible due to differences in exogenously introduced proteins, for example, RFP or β-galactosidase, because the overexpressions of GFP or RFP, which are antioxidants (Palmer et al., 2009) with superoxide radical quenching activities (Bou-Abdallah et al., 2006), have been reported to improve neuronal health. Improved neuronal health caused by less ROS stress may have promoted axonal growth in Figs. 5 and 6. In addition, we used MACS® Neuro Medium supplemented with MACS NeuroBrew®-21, which is an improved version of the minimum essential medium used by Dotti et al. several decades ago, and thus, improved environmental conditions favoring neuronal development may have caused a faster axonal growth rate and contributed to the large axonal length differences observed.

Then what might be the role of NAGK in axons? The first possibility that comes to mind is that NAGK might work as an adaptor protein for dynein-cargo interactions. Cytoplasmic dynein transports diverse cargos by employing adaptors that link dynein complex to specific cargos (Kardon and Vale, 2009). If this is the case, it would be interesting to determine the role played by NAGK in specific trafficking routes, for example, ER to Golgi, Golgi to ER or Golgi to the periphery. This role of NAGK as an adapter is supported by the fact that DYNLRB1 is present in the Golgi compartment and colocalizes with Rab6 GTPase in Neuro-2A Cells (Wanschers et al., 2008). Other members of dynein motor complex, that is, DHC (Roghi et al., 1999) and Tctex-1 (Tai et al., 1998), have also been found in Golgi. NAGK might also link small Golgi particles to DYNLRB1. It has been well noted in non-neuronal cells that small Golgi particles move from the central Golgi clusters to the periphery via dynein motor where Drosophila golgin Lava lamp (Papoulas et al., 2005) and Golgin 160 (Yadav et al., 2012) link Golgi to dynein for movement. However, Dynein might require minus-end out MT orientation in growing axons to carry its cargos towards axonal growth cones. It has been reported that almost all MT plus-ends (99%) are distally oriented in stage 4 axons, but that around 6% are reversely orientated in the growing axons of stage 3 hippocampal neurons (Baas et al. 1989). However, in mouse embryonic cerebral slices (Sakakibara et al. 2014) and in cerebellar granule cells *in vivo* (Rakic et al. 1996) nascent axons were found to contain mixed polarity MTs.

The second possible explanation of the role of NAGK in axons is that it may play a role in acentrosomal MT organizing center. In view of the observed colocalization of NAGK and Golgi at collateral branch extension points and the ends of MTs in axonal growth cones, and the finding by Ori-McKenney et al. (2012) that Golgi outposts act as acentrosomal MT organizing centers, NAGK-Golgi interaction might play a role in MT formation. The non-canonical upregulation of axonal and dendritic growth by NAGK justifies its interactions with many diverse intracellular proteins, such as, DYNLRB1, SnRNPN, and GTF2H5 (Islam et al., 2015; Sharif et al., 2015), although detailed studies of these proteins have yet to be performed. In the present study, we investigated NAGK-DYNLRB1 interaction in rat hippocampal neurons and found that the complex colocalized with small discrete Golgi particles in dendritic branch points and in developing axons. Accumulated evidence on the topic, supported by our findings, establishes that dynein and Golgi contribute to axonal growth. In our opinion, NAGK is a key driver of axonal growth and that the NAGK-dynein-Golgi tripartite interaction explains, to some extent, the mechanism underlying the non-canonical function of NAGK. Our findings also suggest that role played by NAGK in axonal trafficking could be linked with neurodegenerative diseases, such as, amyotrophic lateral sclerosis, Alzheimer's disease, and Huntington's disease, in which early axonal transport dysfunctions have been reported (Gunawardena et al., 2003; Stokin et al., 2005; Trushina et al., 2004; Williamson and Cleveland, 1999).

Note: Supplementary information is available on the Molecules and Cells website (www.molcells.org).

ACKNOWLEDGMENTS

We thank Eun-jung Jung for technical assistance. This research was supported by Basic Science Research Program

through the National Research Foundation of Korea (NRF) funded by the Ministry of Science, ICT and future Planning to ISM (2015R1A2A2A01007104).

REFERENCES

Ahmad, F.J., He, Y., Myers, K.A., Hasaka, T.P., Francis, F., Black, M.M., and Baas, P.W. (2006). Effects of dynactin disruption and dynein depletion on axonal microtubules. Traffic *7*, 524-537.

Baas, P.W., Black, M.M., and Banker, G.A. (1989). Changes in microtubule polarity orientation during the development of hippocampal neurons in culture. J. Cell Biol. *109*, 3085-3094.

Berger, M., Chen, H., Reutter, W., and Hinderlich, S. (2002). Structure and function of *N*-acetylglucosamine kinase. Identification of two active site cysteines. Eur. J. Biochem. *269*, 4212-4218.

Bou-Abdallah, F., Chasteen, N.D., and Lesser, M.P. (2006). Quenching of superoxide radicals by green fluorescent protein. Biochim. Biophys. Acta *1760*, 1690-1695.

Brewer, G.J., Torricelli, J.R., Evege, E.K., and Price, P.J. (1993). Optimized survival of hippocampal neurons in B27-supplemented Neurobasal, a new serum-free medium combination. J. Neurosci. Res. *35*, 567-576.

Dotti, C.G., Sullivan, C.A., and Banker, G.A. (1988). The establishment of polarity by hippocampal neurons in culture. J. Neurosci. *8*, 1454-1468.

Esko, J.D., and Lindahl, U. (2001). Molecular diversity of heparan sulfate. J. Clin. Invest. *108*, 169-173.

Estrada-Bernal, A., Sanford, S.D., Sosa, L.J., Simon, G.C., Hansen, K.C., and Pfenninger, K.H. (2012). Functional complexity of the axonal growth cone: A proteomic analysis. PLoS ONE *7*, e31858.

Gardiol, A., Racca, C., and Triller, A. (1999). Dendritic and postsynaptic protein synthetic machinery. J. Neurosci. *19*, 168-179.

Goslin, K., and Banker, G. (1990). Rapid changes in the distribution of GAP-43 correlate with the expression of neuronal polarity during normal development and under experimental conditions. J. Cell Biol. *110*, 1319-1331.

Goslin, K., Assmussen, H., and Banker, G. (1998). Rat hippocampal neurons in low density culture. In Culturing Nerve Cells, 2nd Ed, Banker, G. and Goslin, K. eds. (Cambridge, MA: MIT Press). pp. 339-370.

Gunawardena, S., Her, L.S., Brusch, R.G., Laymon, R.A., Niesman, I.R., Gordesky-Gold, B., Sintasath, L., Bonini, N.M., and Goldstein, L.S. (2003). Disruption of axonal transport by loss of huntingtin or expression of pathogenic polyQ proteins in Drosophila. Neuron *40*, 25-40.

Hakomori, S. (2000). Traveling for the glycosphingolipid path. Glycoconj. J. *17*, 627-647.

Hinderlich, S., Nöhring, S., Weise, C., Franke, P., Stäsche, R., and Reutter, W. (1998). Purification and characterization of *N*-acetylglucosamine kinase from rat liver: comparison with UDP-*N*-acetylglucosamine 2-epimerase/*N*-acetylmannosamine kinase. Eur. J. Biochem. *252*, 133-139.

Hinderlich, S., Berger, M., Schwarzkopf, M., Effertz, K., and Reutter, W. (2000). Molecular cloning and characterization of murine and human *N*-acetylglucosamine kinase. Eur. J. Biochem. *267*, 3301-3308.

Horton, A.C., and Ehlers, M.D. (2003). Dual modes of endoplasmic reticulum-to-Golgi transport in dendrites revealed by live-cell imaging. J. Neurosci. *23*, 6188-6199.

Horton, A.C., Racz, B., Monson, E.E., Lin, A.L., Weinberg, R.J., and Ehlers, M.D. (2005). Polarized secretory trafficking directs cargo for asymmetric dendrite growth and morphogenesis. Neuron *48*, 757-771.

Hwa, K.Y. (2001). Glycosyl phosphatidylinositol-linked glycoconjugates: structure, biosynthesis and function. Advan. Exp. Mes. Biol. *491*, 207-214.

Islam, M.A., Sharif, S.R., Lee, H.S., Seog, D.H., and Moon, I.S. (2015). *N*-acetyl-*D*-glucosamine kinase interacts with dynein light chain roadblock type 1 at Golgi outposts in neuronal dendritic branch points. Exp. Mol. Med. *47*, e177.

Jareb, M., and Banker, G. (1997). Inhibition of axonal growth by brefeldin A in hippocampal neurons in culture. J. Neurosci. *17*, 8955-8963.

Kardon, J.R., and Vale, R.D. (2009). Regulators of the cytoplasmic dynein motor. Nat. Rev. Mol. Cell Biol. *10*, 854-865.

Lee, H.S., Cho, S.J., and Moon, I.S. (2014a). The non-canonical effect of *N*-acetyl-*D*-glucosamine kinase on the formation of neuronal dendrites. Mol. Cells *37*, 248-256.

Lee, H.S., Dutta, S., and Moon, I.S. (2014b). Upregulation of dendritic arborization by *N*-acetyl-*D*-glucosamine kinase is not dependent on its kinase activity. Mol. Cells *37*, 322-329

Merianda, T.T., Lin, A.C., Lam, J.S., Vuppalanchi, D., Willis, D.E., Karin, N., Holt, C.E., and Twiss, J.L. (2009). A functional equivalent of endoplasmic reticulum and Golgi in axons for secretion of locally synthesized proteins. Mol. Cell. Neurosci. *40*, 128-142.

Moon, I.S., Cho, S.J., Jin, I., and Walikonis, R. (2007). A simple method for combined fluorescence in situ hybridization and immunocytochemistry. Mol. Cells *24*, 76-82.

Ori-McKenney, K.M., Jan, L.Y., and Jan, Y.N. (2012). Golgi outposts shape dendrite morphology by functioning as sites of acentrosomal MT nucleation in neurons. Neuron *76*, 921-930.

Palmer, C.V., Modi, C.K., and Mydlarz, L.D. (2009). Coral Fluorescent Proteins as Antioxidants. PLoS ONE *4(10),* e7298.

Papoulas, O., Hays, T.S., and Sisson, J.C. (2005). The golgin Lava lamp mediates dynein-based Golgi movements during Drosophila cellularization. Nat. Cell. Biol. *7*, 612-618.

Pierce, J.P., Mayer, T., and McCarthy, J.B. (2001). Evidence for a satellite secretory pathway in neuronal dendritic spines. Curr. Biol. *11*, 351-355.

Rakic, P., Knyihar-Csillik, E., and Csillik, B. (1996). Polarity of microtubule assemblies during neuronal cell migration. Proc. Natl. Acad. Sci. USA *93*, 9218-9222.

Reutter, W., Sta¨sche, R., Stehling, P., and Baum, O. (1997). In Glycosciences, Status and Perspectives, H.J. Gabius, and S. Gabius, eds. (Weinheim, Germany: Chapman and Hall Ltd.), pp. 245-259.

Reuter, J.E., Nardine, T.M., Penton, A., Billuart, P., Scott, E.K., Usui, T., Uemura, T., and Luo, L. (2003). A mosaic genetic screen for genes necessary for Drosophila mushroom body neuronal morphogenesis. Development *130*, 1203-1213.

Roghi, C., Allan, V.J., Wall, J.S., and Brown, J.C. (1999). Dynamic association of cytoplasmic dynein heavy chain 1a with the Golgi apparatus and intermediate compartment. J. Cell. Sci. *112*, 4673-4685.

Sainath, R., and Gallo, G. (2014). The dynein inhibitor Ciliobrevin D inhibits the bidirectional transport of organelles along sensory axons and impairs NGF-mediated regulation of growth cones and axon branches. Devel. Neurobio. doi: 10.1002/dneu.22246.

Sakakibara, A., Sato, T., Ando, R., Noguchi, N., Masaoka, M., and Miyata, T. (2014). Dynamics of centrosome translocation and microtubule organization in neocortical neurons during distinct modes of polarization. Cereb. Cortex. *24*, 1301-1310.

Schachter, H. (2000). The joys of HexNAc. The synthesis and function of *N*- and *O*-glycan branches. Glycoconj. J. *17*, 465-483.

Sharif, S.R., Lee, H.S., Islam, M.A., Seog, D.H., and Moon, I.S. (2015). *N*-acetyl-*D*-glucosamine kinase is a component of nuclear speckles and paraspeckles. Mol. Cells *38*, 402-408.

Stokin, G.B., Lillo, C., Falzone, T.L., Brusch, R.G., Rockenstein, E., Mount, S.L., Raman, R., Davies, P., Masliah, E., Williams, D.S., and Goldstein, L.S. (2005). Axonopathy and transport deficits early in the pathogenesis of Alzheimer's disease. Science *307*, 1282-1288.

Tai, A.W., Chuang, J.Z., and Sung, C.H. (1998). Localization of Tctex-1, a cytoplasmic dynein light chain, to the Golgi apparatus and evidence for dynein complex heterogeneity. J. Biol. Chem. *273*, 19639-19649.

Trushina, E., Dyer, R.B., Badger, J.D. 2nd, Ure, D., Eide, L., Tran, D.D., Vrieze, B.T., Legendre-Guillemin, V., McPherson, P.S., Mandavilli, B.S. et al. (2004). Mutant huntingtin impairs axonal trafficking in mammalian neurons *in vivo* and *in vitro*. Mol. Cell. Biol. *24*, 8195-8209.

Van den Steen, P., Rudd, P.M., Dwek, R.A., and Opdenakker, G. (1998). Concepts and principles of O-linked glycosylation. Crit. Rev. Biochem. Mol. Biol. *33*, 151-208.

Wanschers, B., Van de Vorstenbosch, R., Wijers, M., Wieringa, B., King, S.M., and Fransen, J. (2008). Rab6 family proteins interact with the dynein light chain protein DYNLRB1. Cell. Motil. Cytoskeleton *65*, 183-196.

Watanabe, R., Murakami, Y., Marmor, M.D., Inuoe, N., Maeda, Y., Hino, J., Kangawa, K., Julius, M., and Kinoshita, T. (2000). Initial

enzyme for glycosylphosphatidylinositol biosynthesis requires PIG-P and is regulated by DPM2. EMBO. J. *19*, 4402-4411.
Weihofen, W.A., Berger, M., Chen, H., Saenger, W., and Hinderlich, S. (2006). Structures of human *N*-Acetylglucosamine kinase in two complexes with *N*-Acetylglucosamine and with ADP/glucose: insights into substrate specificity and regulation. J. Mol. Biol. *364*, 388-399.
Williamson, T.L., and Cleveland, D.W. (1999). Slowing of axonal transport is a very early event in the toxicity of ALS-linked SOD1 mutants to motor neurons. Nat. Neurosci. *2*, 50-56.
Wolosker, H., Kline, D., Bian, Y., Blackshaw, S., and Cameron, A.M. (1998). Molecularly cloned mammalian glucosamine-6-phosphate deaminase localizes to transporting epithelium and lacks oscillin activity. FASEB J. *12*, 91-99.
Yadav, S., Puthenveedu, M.A., and Linstedt, A.D. (2012). Golgin160 recruits the dynein motor to position the Golgi apparatus. Dev. Cell. *23*, 153-165.